Truncated Airy pulses supercontinuum generation in a silicon-on-insulator optical waveguide including third-harmonic generation and negative-frequency Kerr terms

BOUKAR KEMEDANE SOUANG,[1,3] LUCIEN MANDENG MANDENG,[2,*] CRÉPIN HEUTEU,[1,4] AND CLÉMENT TCHAWOUA[1]

[1]*Laboratory of Mechanics, Materials and Structures, Department of Physics, Faculty of Science, University of Yaoundé I, Yaoundé, Cameroon*
[2]*Department of Mathematics and Physical Sciences, National Advanced School of Engineering, University of Yaoundé I, Yaoundé, Cameroon*
[3]*Department of Physics, University of Adam Barka, Abéché, Chad*
[4]*Centre d'Excellence africain en Technologie de l'Information et de la Communication (C.E.T.I.C), National Advanced School of Engineering, University of Yaoundé I, Yaoundé, Cameroon*
[*]*mandengl@yahoo.fr*

Abstract: We report in this work the numerical study of the supercontinuum generation (SCG) phenomenon raised from femtosecond truncated Airy pulses within a silicon-on-insulator (SOI) waveguide including loss effects, third-harmonic generation (THG) and negative-frequency Kerr (NFK) terms. This study is conducted through a modeling based on the full unidirectional pulse propagation equation (UPPE) model which allows to assume the existence of the NFK term in the Kerr nonlinearity with a spectral filtering. The various effects of the linear loss (LL), the free-carrier absorption (FCA)/ free-carrier dispersion (FCD), the two-photon absorption (TPA), the THG, the NFK, the peak power, the pulse duration and the pulse shape are explored and discussed. For the shape comparison, we use a symmetrical profile of the sech-type pulse. More specifically, we show that the Airy pulse has SCG spectra that are less influenced by the waveguide than the sech-type symmetric pulse; moreover, the losses effectively reduce the spectral intensity (S.I) and the spectral bandwidth (S.B) of the spectra while the THG and the NFK increase them. However, the most deleterious factor for the Airy pulse is the LL, while that of the sech-type pulse is the TPA. The SCG spectra of the Airy pulse are broader and more coherent than that of the sech-type in the studied waveguide. Due to the presence of linear and nonlinear loss terms, the increase in signal energy is deleterious to the SCG in this silicon waveguide; this results in smaller spectra as peak power and pulse duration increase.

1. Introduction

The drastic spectral broadening known as the supercontinuum generation (SCG) and obtained in highly nonlinear media from intense pulses through the combination of both linear and nonlinear processes, has been nowadays extensively investigated [1-11]. The particular attention on the SCG phenomenon has led to numerous applications in nonlinear optics such as biophotonics applications [1,3] (spectroscopy, microscopy, optical coherence tomography, diffuse optical spectroscopy and tomography...), optical frequency metrology [2], optical telecommunications applications [3] (multichannel telecommunication sources in wavelength-division multiplexing systems, pulse compressors...).

In the path of improving more and more the SCG phenomenon, the pulse shaping technique still has a place. It consists in improving the input pulse characteristics for this achievement. This technique encompasses managing the profile, the timewidth, the power or other parameters as the initial chirp [7,12]. In the SCG studies, the overwhelming majority of prior studies already cited above [1-6,8,9] utilized intense optical pulses with symmetric and compact temporal profiles such as Gaussian or sech-type pulses while the only ones that focused on Airy pulses are those of refs. [7,10,11,13]. One should remind that, Airy pulses are first predicted by Berry and Balazs within the context of quantum mechanics [14] and, their first introduction in nonlinear optics followed in 2007 by Siviloglou and Christodoulides [15]. The Airy waves have special properties that have been already studied leading to several applications [16-39].

On the other hand, among the highly nonlinear waveguides investigated for the SCG phenomenon figure the non-silica fibers. The silicon waveguides belong to this category of waveguides [40]. This material enhances the tight confinement of optical pulses in the sub-micro wavelengths region when one uses the silicon-on-insulator (SOI) technology [41]. It offers a Kerr coefficient of nonlinearity hundred times the one of silica while its Raman gain is one thousand times the one of silica [40]. Consequently its nonlinear properties are enhanced compared with those of silica and they allow an efficient nonlinear interaction for short waveguide lengths as below 5 cm. Nonetheless, the limiting factors of SOI-waveguides are defined as the two-photon absorption (TPA), the free-carrier absorption (FCA) and the free-carrier density (FCD). The SOI-waveguides have various applications [40-46].

The effects of TPA, FCA/FCD have already been analyzed on the broadened spectra induced by the SCG [41,43] and by the SPM only [47,48]. Indeed, for instance in ref. [43], the TPA was shown to reduce significantly the spectral bandwidth (SB). Moreover, for ultrashort pulses as those in the sub-picosecond domain (femtosecond pulses) for which the effective carrier lifetime should be neglected, Yin et al demonstrated that neither stimulated Raman scattering (SRS) nor FCA/FCD plays a significant role during the SCG in SOI-waveguides [43]. Furthermore, nonlinear multiphoton absorptions (NMAs) processes play a crucial role in limiting the transparency of optical window materials and in causing laser-induced damage to optical components, particularly at short wavelengths [10,11,47-52]. The NMAs processes have been successfully used to produce population inversion in semiconductor laser materials [49].

More recently, the impact on the self-phase modulation (SPM) of both the third-harmonic generation (THG) phenomenon and a novel one dubbed negative-frequency Kerr (NFK) effect, were studied in a Kerr medium [53]. In this study, Loures et al found that, the THG induces additional symmetric lobes in the SPM-broadened spectrum while the amplitude of these sidebands are importantly increased by the NFK term and the self-steepening (SS) effect. The NFK was first discussed theoretically in ref. [54] after the pioneers experiments done in refs. [55-57] and that have revealed the possibility of solitons to emit such negative-frequency resonant radiation. Furthermore, Conforti et al showed that the NFK term does not appear in the common generalized nonlinear Schrödinger equation (GNLSE) based on the slowly-varying envelope approximation (SVEA), and they modeled subsequently a new equation based on the full unidirectional pulse propagation equation (UPPE) that includes the NFK in a GNLSE-like form [54]. It is well-known that, the THG as the four-wave mixing (FWM) necessitates a phase-matching condition to occur in a Kerr medium [2,58,59]. This is not in general satisfied for standard single-mode fibers while phase-matching is much easier to accomplish in highly nonlinear waveguides [2].

Assuming that SOI-waveguides are media that possess high values of Kerr nonlinearity, the consideration of the THG effect could be set. If the analytical modeling of the propagation within SOI-waveguides is not conducted through the SVEA but rather through the novel modeling introduced in ref. [54], the NFK term could also been included. The question of such considerations has not yet been formulated until now for SOI-waveguides. Indeed, we set opened existing interrogations as : (i) is there an existing modeling of pulse propagation within SOI-waveguides that combines SPM, SS, TPA, THG and NFK ? (ii) What happen to the truncated Airy pulse SCG when all these effects are investigated together ? (iii) What about its coherence properties ?. It should be noted that the characteristics of the Airy pulses have already been studied in the context of SOI waveguides [22-24,60,61] but not in the context of the SCG (except for other kinds of waveguides [7,10,11]) and even more in the consideration of the terms of multiphoton absorption with the terms NFK and THG.

In this work, we conduct for the first time to the best of our knowledge, a modeling that combines into a nonlinear equation the aforementioned nonlinear effects for a SOI-waveguide. This modeling relies on both the one of ref. [40] and the one of ref. [54]. Then, we derive the corresponding equation used to generate numerically by a modified adapted version of the MATLAB code provided in ref. [62], the SCG spectra. Since the single impacts of the SPM, TPA, FCA/FCD, NFK, and THG terms on the spectra are known [1,2,43,47,48,53], we focus in this work on their influence upon the properties of the SCG obtained through the truncated femtosecond Airy pulses in a SOI-waveguide. A particular attention is given to the linear losses, FCA/FCD, TPA, THG, the NFK, and the pulse characteristics such as the peak power, the duration and the shape.

This paper is organized as follows : section 2 describes the analytical modelling of the studied system; the results obtained are presented in section 3 while section 4 highlights the features raised from these findings. A conclusion is done at the last section.

2. Modelling

The SOI-waveguide studied in this work is designed as shown in Fig.1 of ref. [41] which has been provided here in Fig. 1. The pumping is done at the optical telecommunication wavelength

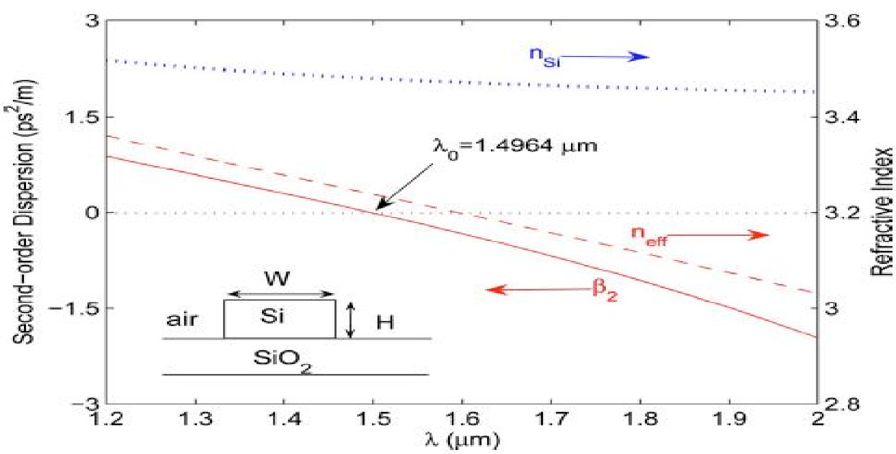

Fig. 1. (color online) Description of the waveguide. Figure 1 reprinted with permission from L. Yin, Q. Lin, and G. P. Agrawal, Opt. Let. **32**, 391 (2007) [41], https://doi.org/10.1364/OL.32.000391. Copyright 2007 by the Optica Publishing Group.

$\lambda_0 = 1.55$ μm. The waveguide has the following data for the fundamental TE mode : the width $W = 0.8$ μm and the height $H = 0.7$ μm [41]; For the analytical modelling, let us start with the full UPPE expressed as follows [54]:

$$i\frac{\partial \tilde{E}(z,\omega)}{\partial z} + \beta(\omega)\tilde{E}(z,\omega) + \frac{\omega}{2cn(\omega)}\tilde{P}_{NL}(z,\omega) = 0. \quad (1)$$

It is a reduction of the Maxwell's equations which accounts only for the forward propagating part of the electric field $E(z,T)$, with $\tilde{E}(z,\omega)$ being its Fourier Transform (FT). The parameters $n(\omega)$, c and $\tilde{P}_{NL}(z,\omega)$ are the linear refractive index, the speed of light in the vacuum, and the FT of the electric nonlinear polarization, respectively. The function $\beta(\omega)$ is the propagation constant which is commonly expanded in Taylor series generating the chromatic dispersion profile (CDP) of the waveguide [2]. Then, one introduces the pulse envelope that deals with the detuning frequency $\Delta\omega$ from the pump frequency ω_0 as $\omega_0 \pm \Delta\omega$. Nonetheless, contrary to the SVEA approach where $|\Delta\omega| \ll \omega_0$, here we consider rather $supp\{\Delta\omega\} \in [-\omega_0; +\infty[$ so that one could obtain negative frequencies [54]. It is therefore a spectral extension of the SVEA. The electrical field is defined as $E(z,T) = u(z,T)exp\big[i(\beta_0 z - \omega_0 T)\big]$ where $u(z,T)$ is its amplitude. With such hypotheses, one derives the following temporal nonlinear polarization [54]:

$$P_{NL}(z,T) = \frac{3\chi^{(3)}}{8}\Big[\frac{1}{3}\big(u^3(z,T)exp(3i\theta)+u^{*3}(z,T)exp(-3i\theta)\big)+|u(z,T)|^2\big(u(z,T)exp(i\theta)+u^*(z,T)exp(-i\theta)\big)\Big], \tag{2}$$

where $\theta = -\omega_0 T + \beta_0 z$, $u^3(z,T)exp(3i\theta)$ accounts for the THG of positive frequencies, $u^{*3}(z,T)exp(-3i\theta)$ accounts for the THG of negative frequencies, $|u(z,T)|^2 u(z,T)exp(i\theta)$ is for the well-known positive frequencies cubic Kerr nonlinearity inducing the SPM, and $|u(z,T)|^2 u^*(z,T)exp(-i\theta)$ corresponds to the novel term dubbed as cubic NFK effect [53,54]. Introducing Eq. (2) in Eq. (1) yields after a cumbersome calculation the following nonlinear partial differential equation (PDE) in the retarded frame of time T following the propagation distance z :

$$\begin{aligned} i\frac{\partial u(z,T)}{\partial z} + \sum_{k=2}^{k=10}\frac{i^k\beta_k}{k!}\frac{\partial^k u(z,T)}{\partial T^k} =& -\gamma'(1+i\tau_{shock}\frac{\partial}{\partial T})u(z,T)\Bigg[\big(|u(z,t)|^2 + a_{NFK}(u^*(z,T))^2 exp(2i\phi) \\ &+ \frac{a_{THG}}{3}(u(z,T))^2 exp(-2i\phi)\big)\Bigg]_+ - \frac{i}{2}(\alpha_l + \alpha_f)u(z,T), \end{aligned} \tag{3}$$

with β_k, τ_{shock}, ϕ, a_{NFK}, a_{THG}, α_l and α_f being the k^{th} coefficient of the CDP, the shock parameter (or SS effect), the phase (defined as $\phi = \omega_0 T + \Delta k z$ [54]), the NFK coefficient, the THG coefficient, the linear losses and the FCA, respectively. The subscript $'+'$ prescribes that only positive frequencies must be taken (i.e. $\Delta\omega > \omega_0$) and is a shorthand notation to indicate the positive frequency *spectral filtering* involved in the analytic signal, and operated in the time domain by the Hilbert transform, which is crucial in this formulation according to ref. [54]. Such operation is important when the sub-cycle pulses are considered assuming that for them, the common SVEA is completely invalid [54]. The coefficient of the cubic nonlinearity is defined in the SOI-waveguide by $\gamma' = \gamma + i\Gamma_{TPA}$ where $\gamma = 2\pi n_2/\lambda_0 A_{eff}$ is the cubic Kerr coefficient and $\Gamma_{TPA} = \beta_{TPA}/2A_{eff}$ the TPA parameter both of them well defined in refs. [40,41,48]. The parameters $n_2 = 6\times10^{-18}\ m^2/W$ and $A_{eff} = 0.32\ \mu m^2$ are respectively the nonlinear index and the effective area of the waveguide. One obtains $\gamma \approx 76\ W^{-1}m^{-1}$ and $\Gamma_{TPA} \approx 7.8125\ W^{-1}m^{-1}$ at the pumping wavelength. The linear losses α_l are taken with the value 2 $dB.cm^{-1}$ at the considered pumping wavelength [63,64] while the FCA $\alpha_f = \sigma N_C \delta$ where $\sigma = 1.45\times10^{-21}\ m^2$ for silicon and N_C accounts for the FCD defined with the growth rate equation as $\partial N_C/\partial T = \left(\beta_{TPA}\lambda_0|u(z,T)|^4/2hcA_{eff}^2\right) - N_C/\tau$ with τ being the effective carrier lifetime [41,63]. We introduce the parameter $\delta = 1 + i\mu$ where μ is well-defined in ref. [64] as $\mu = 2k_c\omega_0/\sigma c$ with $k_c = (8.8\times10^{-28}N_C + 1.35\times10^{-22}N_C^{0.8})/N_C$. In silicon, $\tau \approx 3\ ns$ leading the related term to be neglected for femtosecond pulses used here at relatively low repetition rates and consequently the FCD parameter has been calculated and approximated with an Euler integration scheme as $N_C^{Airy} \approx 3.4180\times10^{22}\ m^{-3}$ for Airy pulses and $N_C^{sech} \approx 6.3356\times10^{22}\ m^{-3}$ for sech-type pulses with the pulse duration $t_0 = 50\ fs$ and its peak power $P_0 = 50\ W$. To have significant THG and NFK in the process, we proceed with a nonzero spatial phase $\phi = \Delta k z$ assuming a matching of frequencies as discussed in Eqs. 10.1.5 and 10.1.6 of ref. [2]. Thus, $\Delta k = \beta_1(\lambda_0)\omega_0 - \beta_0(\lambda_0)$ where $\beta_1(\lambda_0) = (1/c)\Big[n_{Si}(\lambda_0) - \lambda_0\big(dn_{Si}(\lambda)/d\lambda\big)|_{\lambda=\lambda_0}\Big]$ with

$\omega_0 = 2\pi c/\lambda_0$; $n_{Si}(\lambda)$ is the refractive index of silicon at the wavelength λ. It is calculated from the Sellmeier-type equation [41,65]:

$$n_{Si}(\lambda) = \sqrt{1 + \frac{c_1\lambda^2}{\lambda^2 - \lambda_1^2} + \frac{c_2\lambda^2}{\lambda^2 - \lambda_2^2}}, \tag{4}$$

where $c_1 = 9.733$, $c_2 = 0.936$, $\lambda_1 = 290.4\ nm$ and $\lambda_2 = 366.9\ nm$. After a small calculation, we obtain $\Delta k = -2\pi dn_{Si}(\lambda)/d\lambda|_{\lambda=\lambda_0} = 4.966576349 \times 10^5\ m^{-1}$ at $\lambda_0 = 1550\ nm$. The coefficients a_{NFK} and a_{THG} can take the values 0 or 1, depending which nonlinear terms (between NFK and THG) one wishes to activate or not [53]. Considering the development described above, the model PDE solved in the SCG numerical code is given by [3]:

$$i\frac{\partial\tilde{u}(z,\omega)}{\partial z} = -\bar{\gamma}' exp(\hat{L}(\omega)z)F\left\{\bar{u}(z,T)\left[|u(z,t)|^2 + a_{NFK}(u^*(z,T))^2 exp(2i\phi) + \frac{a_{THG}}{3}(u(z,T))^2 exp(-2i\phi)\right]\right\}_+. \tag{5}$$

The function $\hat{L}(\omega)$ is the linear operator and $F\{\}$ the FT operator [2,3,62]. The linear operator $\hat{L}(\omega)$ includes the linear losses α_l, the FCA α_f (which includes the FCD), and the CDP coefficients. We use a truncated Airy pulse profile given as $u(0,T) = \left(P_0\right)^{1/2} Ai\left(T/t_0\right) exp\left(aT/t_0\right)$ with $Ai(\tau)$ and a being the Airy function and the truncation coefficient, respectively. The truncation coefficient or decay factor a ($0 < a < 1$) is a quantity to ensure containment of the infinite Airy tail and can thus enable the physical realization of such pulses [36]. In practice, an Airy pulse can be produced by adding a cubic phase to a Gaussian spectrum [7,35,36]. The truncation coefficient is taken as $a = 0.05$. The CDP of the considered SOI-waveguide is defined as $\beta_2 = -0.1701\ ps^2/m$ [41], $\beta_3 = 0.008505\ ps^3/m$, $\beta_4 = -0.42525 \times 10^{-3}\ ps^4/m$, $\beta_5 = 0.212625 \times 10^{-4}\ ps^5/m$, $\beta_6 = -0.1063125 \times 10^{-5}\ ps^6/m$, $\beta_7 = 5.315625000 \times 10^{-8}\ ps^7/m$, $\beta_8 = -2.657812500 \times 10^{-9}\ ps^8/m$, $\beta_9 = 1.328906250 \times 10^{-10}\ ps^9/m$, $\beta_{10} = -6.644531250 \times 10^{-12}\ ps^{10}/m$, obtained with Eq. (7) of ref. [6].

To explore the coherence degree (CD) of the obtained spectra, we calculate the first-order CD given as [1-3,5,7,8,66,67]:

$$\left|g_{12}(\lambda, T_1 - T_2)\right| = \frac{|\langle u_1^*(\lambda,T_1)u_2(\lambda,T_2)\rangle|}{\sqrt{\left\langle|u_1(\lambda,T_1)|^2\right\rangle\left\langle|u_2(\lambda,T_2)|^2\right\rangle}}, \tag{6}$$

where $u_1(\lambda, T_1)$ and $u_2(\lambda, T_2)$ are the envelope amplitude (with a given shape) of two propagating electric fields of independently SCG pairs. These electric fields belong to immediately successive generated SCG spectra. The CD function is bordered as $0 \leq \left|g_{12}(\lambda, T_1 - T_2)\right| \leq 1$. The value 0 corresponds to totally incoherent spectrum while the maximal value 1 deals with the perfect spectral coherence. We have calculated the CD function in order to focus on the wavelength dependence of the coherence.

Our results are obtained using the MATLAB software run on two computers : Intel(R) Core(TM) i7-2760QM CPU @ 2.40GHz (8 CPUs), 2.4GHz and 8GB of random access memory and a quad-core (Intel Pentium Gold G5500 CPU @3.80 GHz) computer. The numerical code is based on the well-known split-step Fourier method (SSFM) [2,3]. We have modified and re-adapted the MATLAB code kindly provided in ref. [62] by J.C. Travers, M. H. Frosz and J. M. Dudley. We have modified the command lines according to the specificities of our work (please consider the supplementary material).

With all these modifications (view the supplement document of this paper) within the MATLAB code provided in ref. [62], we obtain the results in the following section.

3. Numerical results

3.1. Effects the waveguide parameters on the SCG

We start to show in Fig. 2, the single effects of the waveguide parameters on the SCG phenomenon of truncated Airy pulses (consider Fig. 2(a.1) to Fig. 2(d.1)). A comparison is done with the sech-type pulse which is the ideal candidate for symmetric pulses (consider Fig. 2(a.2) to Fig. 2(d.2)). The isolated effects of the parameters of the waveguide are investigated by considering one parameter after another, i.e. when, for example, the effect of linear losses (LL) is studied ($\alpha_l \neq 0$), all the other parameters are canceled and so on. The effect of LL alone is described by the solid black curves, that of FCA ($\alpha_f \neq 0$) is described by the blue curves in dashed lines; the dotted purple curves describe the TPA ($\Gamma_{TPA} \neq 0$) effect alone while the THG ($a_{THG} = 1$) is drawn by the green dot-dash curves, and finally the red dotted curves are for the NFK ($a_{NFK} = 1$). For realistic SOI-waveguides (very short waveguides) of the order of a centimeter, we have illustrated on the LHS of Fig. 2 the results at $z = 1$ cm and to see how the various effects are accentuated according to the propagation distance, we have gone up to 7 cm for the RHS results of Fig. 2. When we are interested in the LL effect, the observation of the solid black curves at 7 cm shows that it is the most deleterious parameter for the SCG of the Airy followed by the FCA and TPA which are substantially similar in terms of reduction impact (see Figs. 2(b.1) and 2(d.1)). THG and NFK, on the other hand, are more favorable to spectral spreading (see the green and red curves in Fig. 2(b.1)). It can be seen that at 1 cm only the LL has a relatively perceptible effect on the SCG (see Figs. 2(a.1) and 2(c.1)) while the other parameters have approximately the same impact which is not very significant. Thus, the effects increase with propagation distance when comparing 2(a.1) and 2(c.1) with 2(b.1) and 2(d.1). As already discussed in ref. [7,13], the spectral profile of the Airy pulse is a Gaussian shape (see the curves in Fig. 2(a.1) and 2(b.1)). Overall when looking at Figures 2(a.1) to 2(d.1), it can be seen that linear and nonlinear losses (LL, FCA and TPA) have the expected effect of reducing the spectral intensity (S.I) as well as the spectral bandwidth (S.B) of the truncated Airy pulse. By focusing on the time domain of figures 2(c.1) for 1 cm and 2(d.1) for 7 cm, we see that with the propagation distance solitonic fission (SF) is drastically realized.

The comparison of these effects on another pulse profile which is rather symmetric like the sech-type (Figs. 2(a.2) to 2(d.2)), shows that these different parameters affect more this type of pulse than airy pulse. Indeed, we see here that from 1 cm (see 2(a.2) and 2(c.2)), the different impacts of the parameters are distinct from each other. Here, the TPA is the most deleterious effect followed by the LL and FCA while obviously the THG and the NFK act rather in the direction of improvement of the SCG as for the Airy pulse.

At the end of this subsection, it can be seen that the losses, whether linear or nonlinear, reduce as expected the S.I and S.B of the symmetrical (sech-type) and asymmetrical (Airy) pulses while the THG and NFK as terms rather, nonlinear terms related to SPM spread the spectrum in order to improve it. However, the influence on these two profiles is not the same. For short distances, the asymmetrical Airy pulse resists well to the impact of the waveguide in the SCG phenomenon, which is not the case for the symmetrical pulse of the sec-type. TPA reduces sech-type pulse more than Airy pulse, whereas LL affects the latter more.

3.2. Comparison between the truncated Airy and sech-type pulses

To see how the two pulses behave under the same conditions of the single effects for the various parameters discussed above, we have superimposed them on Fig. 3. The general observation made on these cases represented in figure 3 for the two types of profile consists in that the spectra of the Airy pulse are clearly broader than those of the sech-type pulse (see the first and the third rows 3(a.1) to 3(e.1) for $z = 1$ cm and $z = 7$ cm, respectively). We also see that non-solitonic radiation (NSR) is emitted under the influence of THG and NFK but more explicitly

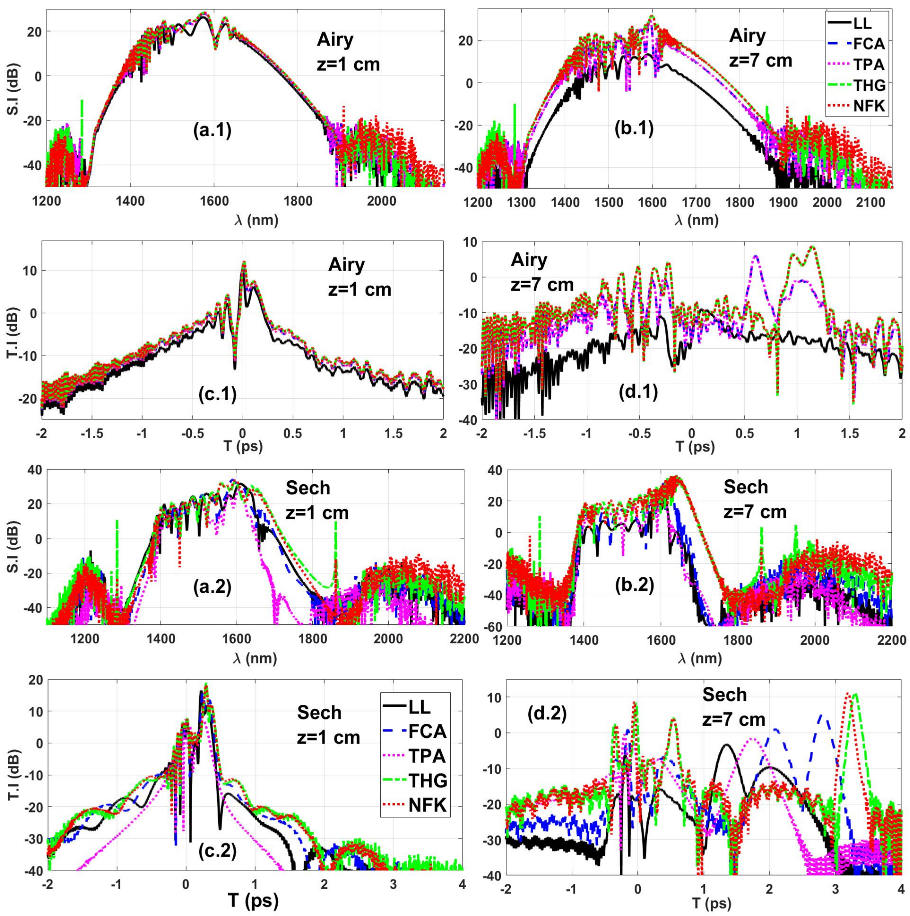

Fig. 2. (color online) For all : $P_0 = 50\ W$, $t_0 = 50\ fs$ at the pumping wavelength 1550 nm. Plots of left-hand side (LHS) are for $z = 1\ cm$ and those of right-hand side (RHS) are for $z = 7\ cm$. From (a.1) to (d.1) are for Airy pulse and from (a.2) to (d.2) are for the sech-type pulse. (a.1), (b.1), (a.2) and (b.2) are for the SCG spectra while (c.1), (d.1), (c.2) and (d.2) are for the temporal output profiles.

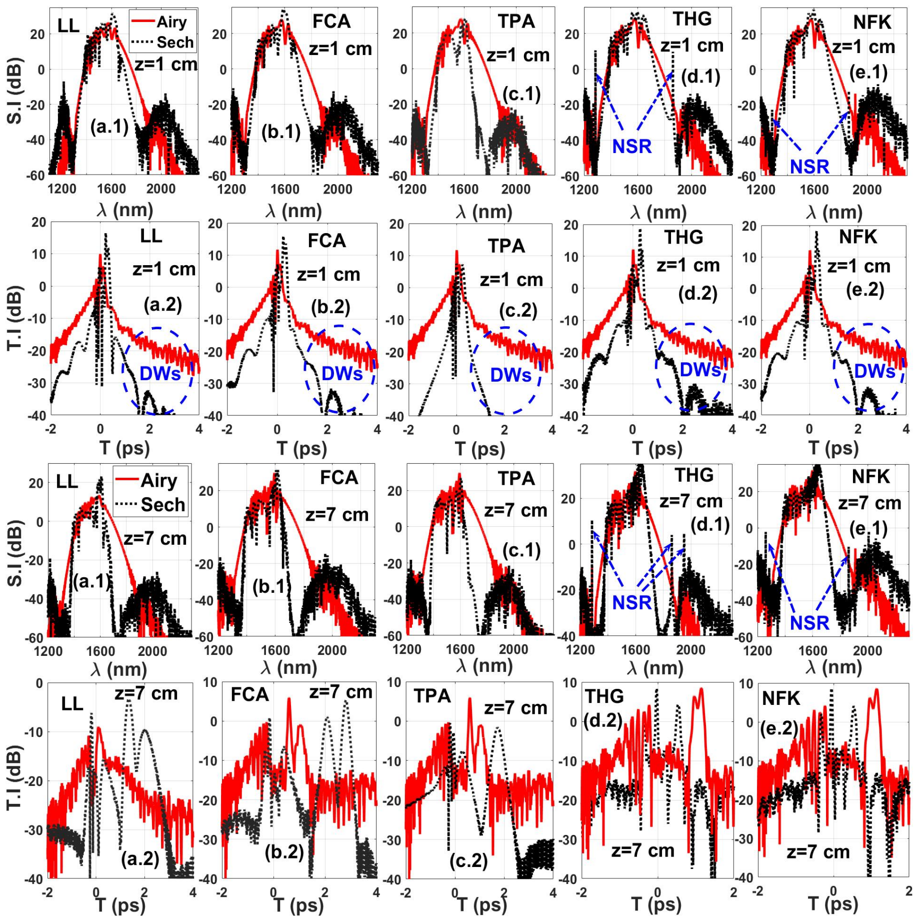

Fig. 3. (color online) Same conditions as in Fig. 2. Top figures (a.1) to (e.1) and (a.2) to (e.2) are for $z = 1$ cm. Bottom figures (a.1) to (e.1) and (a.2) to (e.2) are for $z = 7$ cm. Red solid curves are for truncated Airy pulse while black dashed curves are for sech-type pulse.

on the sech-type pulse than on the Airy pulse (see 3(d.1) and 3(e.1) at the first and third rows). Moreover, in the time domain, the extent of the zone as well as the intensity of the dispersive waves (DWs) are more important for the Airy pulse at low propagation distances ($z = 1$ cm, see the curves of the second row 3(a.2) to 3(e.2)) than for the sech-type pulse. The discussion around the emission of DWs and NSRs during the SCG phenomenon by pulses has been extensively done in refs. [54-57,68].

3.3. Full case

In the full case in which all the parameters studied above (LL, FCA, TPA, THG and NFK) are considered as non-zero simultaneously, we have produced Figure 4. The first and second lines are for $z = 1$ cm while the third and fourth lines are for $z = 7$ cm.

For the two pulses, this more realistic case of the studied silicon waveguide demonstrates that the linear and nonlinear absorption terms, in particular the LL, the FCA and the TPA, are preponderant in the progress of the SCG. Indeed, it is observed that the spectra diminish as the propagation distance increases (see the figures in the first column). Obviously the observation made in Figure 3 is also made here, namely that the S.B of the Airy pulse is significantly larger than that of the sech-type (See Figs. 4(c.1) and 4(c.2)); for example we have approximately at

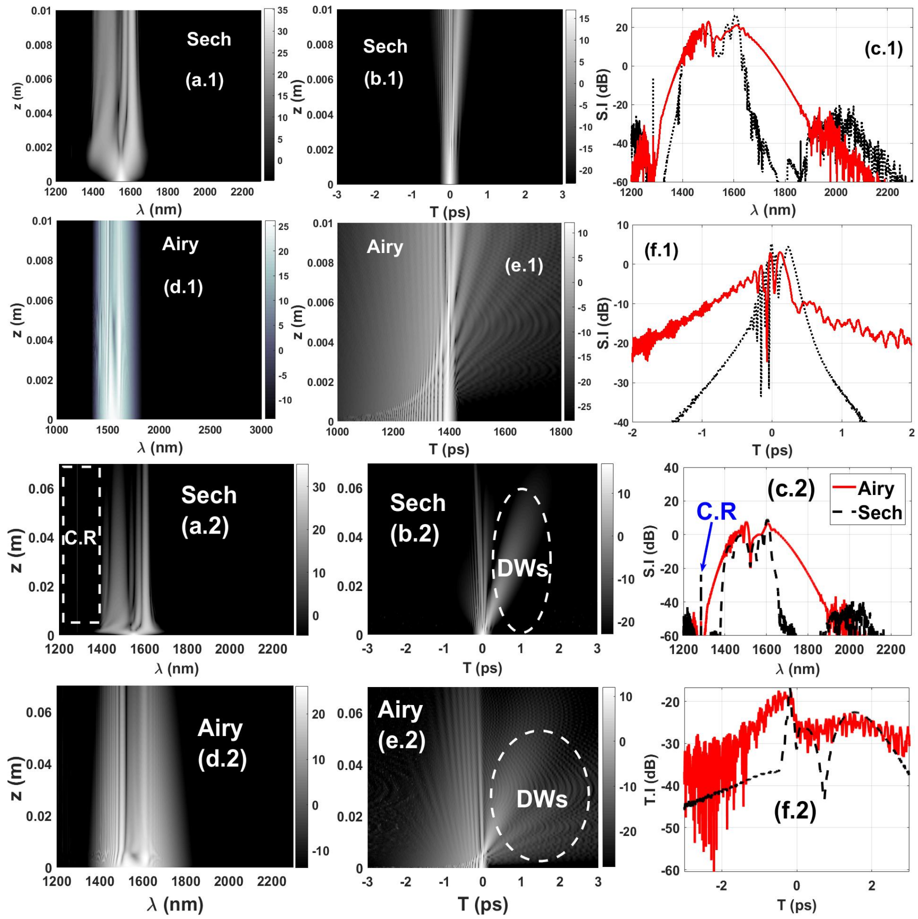

Fig. 4. (color online) Same conditions as in the previous figures 2 and 3. Now all the parameters studied above are all taken together non-zero simultaneously to constitute the full case.

-20 dB, 500 nm for the Airy against approximately 267 nm for the dry at $z = 1$ cm (see Fig. 4(c.1)).

Along with the propagation distance, the nonlinear terms of THG and NFK cooperate to generate the NSR known as the Cherenkov radiation (C.R) for the sech-type pulse (see Figs. 4(a.2) and 4(c. 2)). The reduction induced by LL, FCA and TPA does not change the ratio between the two S.Bs of the two pulses (see Fig. 4(c.2)). Still at -20 dB, we note that in S.B, we have approximately 400 nm for the Airy and approximately 220 nm for the sech-type pulse. The ratio of S.Bs to -20 dB is obtained approximately around 0.5; thus under the same conditions in the waveguide considered, the Airy pulse seems to produce a spectrum twice as large as that of the sech-type. The DWs are emitted intensely the longer the propagation distance increases (see Figs. 4(b.2) and 4(e.2)). Obviously, this is done with more magnitude for the Airy pulse than for the sech-type pulse as discussed in Figure 3 (second row).

It emerges from these results that the silicon waveguide like the conclusions of ref. [41] absorbs a good part of the propagating signal through its loss terms, as the distance increases. This induces a reduction of the S.I and the S.B. Nevertheless, the Airy pulse is quite resistant to this deleterious impact and still produces a relatively broader spectrum than that of the sech-type. Furthermore, the shedding of the DWs is more accentuated in the Airy than in the sech-type pulse, while the latter undergoes more the shedding of the C.R in comparison to the Airy under the same conditions. We can deduce that the robustness, the resistance in propagation of the Airy would be at the origin of such features. Which robustness is intrinsically linked to the distribution of the energy of said pulse in its various lobes: from the dominant to the secondary lobes of the tail oscillations.

3.4. Pulse characteristics: effects of peak power and pulse duration

Let us now consider the the characteristics of the pulses, in particular the peak power P_0 and the pulse duration t_0. These magnitudes were varied from values 25 to 100 respecting a step of 25 each time.. The obtained results are depicted in Fig. 5. By observing figures 5(a.1), (b.1), (a.2)

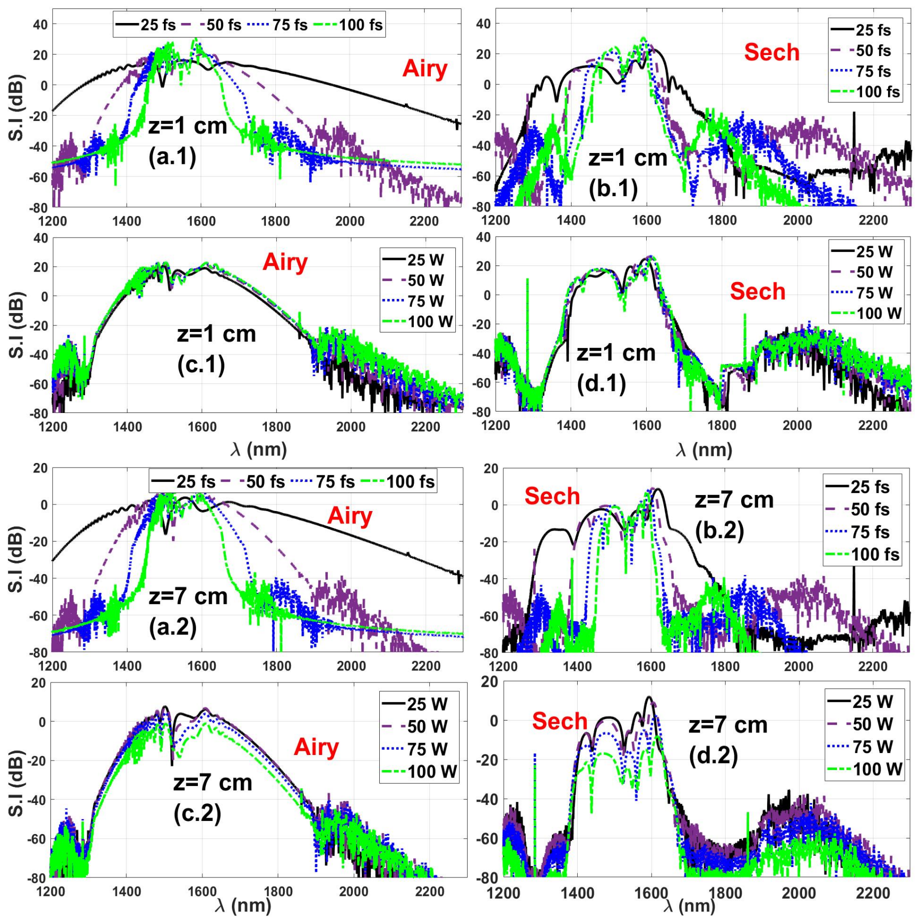

Fig. 5. (color online) The conditions are the same as in the full case of Fig. 4 except that here P_0 or t_0 are varied implying that the FCA should be recalculated each time for each following the pulse shape using the Euler integration scheme of the growth rate equation mentioned above in section 2.

and (b.2) where the pulse duration has been varied for the two pulses, we see that the more the duration is smaller, the larger the S.B. The S.B is therefore inversely proportional here to the duration of the pulse and that, for the two types of profile. This result is surprising and contradicts the discussion made in ref. [1] about the influence of t_0 on the SCG phenomenon. Indeed, when we consider figure 16 of ref. [1] on page 1157 of said article, we see that the increase in S.B in the SCG is proportional to the increase in t_0. Contrary to this result, we here in the SOI-waveguide, we observe the opposite. In the principle of ref. [1], the number of input solitons is related to the pulse duration t_0, and therefore since the S.F occurs during the SCG, then the higher the number of solitons (implying t_0) the greater is the S.B. This is certainly caused by the presence of the absorption terms which particularly affect signals filled with energy. Since if we increase the pulse duration while keeping the peak power constant, this induces an increase in the energy of the pulse, thus making it vulnerable to losses (LL, FCA and TPA).

To confirm our assertion, we also plotted the spectra by varying the peak power instead of the pulse duration (consider figures 5(c.1), (d.1), (c.2) and (d.2)). We see for example in the figures of $z = 7\ cm$ in 5(c.2) for the Airy pulse and 5(d.2) for the dry-type pulse, that the width of the S.B of $P_0 = 100\ W$ is significantly smaller than that of $P_0 = 25\ W$. It is therefore observed that the most energetic signals generate here in the long run, smaller spectra. This contrasts with the results known so far about the energization of pulses at the input of waveguides to perform the SCG. In fact, one of the common methods to improve the SCG via the input pulse is to energize it more in the expectation of a more vigorous interaction with the waveguide producing a spectral explosion in terms of S.B. [1-4]. But here we show that for waveguides such as those in silicon which have significant linear and nonlinear losses, it is rather disadvantageous to increase the energy of the signals. This is what emerges from figure 5, regardless of the type of shape of the pulse.

3.5. SCG spectral coherence

To assess the quality of the spectra obtained as a function of the different parameters, we used equation (6) according to refs. [5,66,67] by making two twin signals u_1 and u_2 interact in an autocorrelation, one of which is normal and the other noisy in order to define the CD $|g_{12}(\lambda)|$ which is between 0 and 1. The value 1 is for a perfect consistency of the spectrum and 0 for a totally noisy spectrum. Figure 6 was obtained for the different parameters. As shown in this

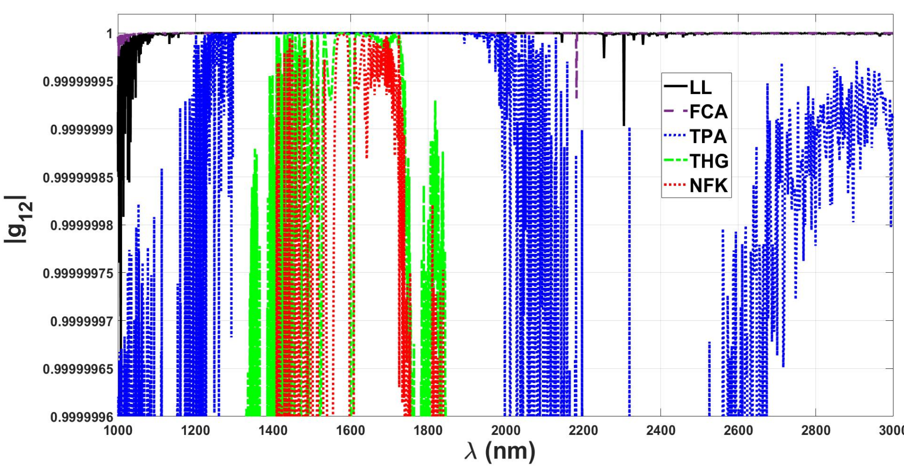

Fig. 6. (color online) For all $z = 1\ cm$, $P_0 = 50\ W$ and $t_0 = 50\ fs$ with $\lambda_0 = 1550\ nm$.

figure, we can conjecture that the spectral coherence according to the various parameters follows the following order: the spectrum is more coherent under the LL alone (dashed purple curve) then under the FCA alone (solid black curve), followed by TPA (blue dotted curve), THG (green dot-dash curve) and NFK (dotted red curve) being the last one because giving the least coherent spectrum of all.

By zooming in on the CD obtained under the same conditions for the Airy pulse and the dry-type pulse in Figure 7(I), we see that the spectrum of the Airy pulse is clearly more coherent than that of the dry-type. Likewise, it is observed in FIG. 7(II) that the high power decreases the

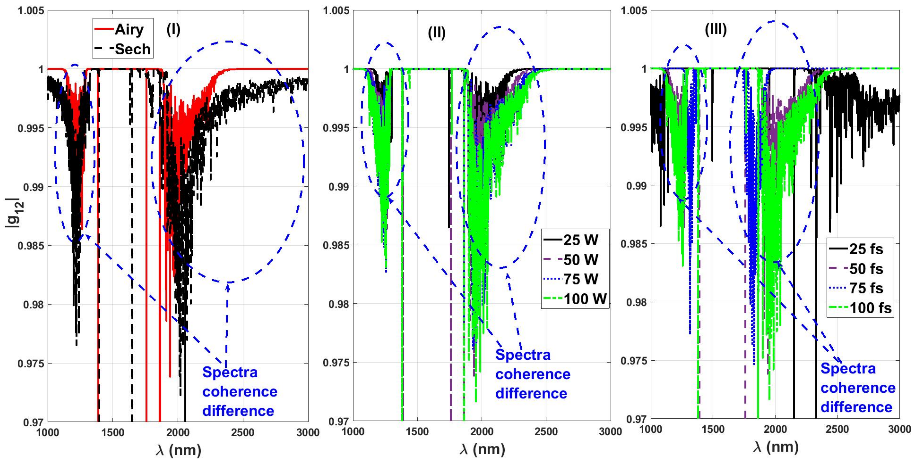

Fig. 7. (color online) For all $z = 1\ cm$. Plots of CD versus the wavelength for the characteristics of the pulse: (I) for the shape, (II) for the peak power with the Airy pulse, (III) for the pulse duration with the Airy pulse.

spectral coherence. Moreover, in Figure 7(III) the Airy pulse having a duration of 100 fs has a less coherent spectrum than that of 50 fs. Thus, the longer the pulse, the less it has coherent spectra in the waveguide studied.

4. Highlights

The hotspots of this work are summarized in this section following the findings discussed above:

- the Airy pulse has a SCG spectrum that is less influenced by the waveguide than the sech-type symmetric pulse,
- the losses effectively reduce the S.I and the S.B of the spectra while the THG and the NFK increase them. However, the most deleterious factor in this sense for the Airy pulse is the LL, while that of the sech-type pulse is the TPA,
- the spectrum of the Airy pulse is broader than that of the sech-type in the studied waveguide,
- the intensity and area extent of the DWs are more important for the Airy pulse than the sech-type,
- the C.R is generated in the sech-type pulse because its spectrum is more affected by THG and NFK,
- due to the presence of linear and nonlinear loss terms such as LL, FCA and TPA, the increase in signal energy is deleterious to the SCG in this silicon waveguide; this results in smaller spectra as peak power and pulse duration increase. This result contrasts with that of ref. [1] because in this case, we consider the absorptions which are not present in the waveguide of [1]. We define the relations $S.B \propto 1/P_0$ and $S.B \propto 1/t_0$,
- the spectral coherence defined by the CD was found to be related to the previous result, i.e. when the pulse has more energy, the coherence decreases and therefore for the Airy pulse:

$$
\begin{aligned}
&\left|g_{12}^{LL}\right| > \left|g_{12}^{FCA}\right| > \left|g_{12}^{TPA}\right| > \left|g_{12}^{THG}\right| > \left|g_{12}^{NFK}\right|, \\
&\left|g_{12}\right| \nearrow\ with\ P_0 \searrow, \\
&\left|g_{12}\right| \nearrow\ with\ t_0 \searrow,
\end{aligned}
\tag{7}
$$

- the Airy pulse has a spectral coherence above that of the sech-type pulse: $\left|g_{12}^{Airy}\right| > \left|g_{12}^{sech}\right|$.

Thus, the suggestion at the end of this work is that for the realization of an optimal and more coherent SCG under the conditions described in this paper, the choice of an Airy pulse with short duration and low peak power is more suitable.

5. Conclusion

In short, we have numerically studied in this work the SCG phenomenon raised from femtosecond truncated Airy pulses within a SOI-waveguide including loss effects, THG and NFK terms. This study was conducted through a modeling based on the full UPPE model which allows after refs. [41,54] to assume the existence of the NFK term in the Kerr nonlinearity with a spectral filtering. The various effects of the linear losses, the FCA/FCD, the TPA, the THG, the NFK, the peak power, the pulse duration and the pulse shape have been explored and discussed. For the shape comparison, we used a symmetrical profile of the sech-type. More specifically, we have shown that the Airy pulse has SCG spectra that are less influenced by the waveguide than the sech-type symmetric pulse; moreover, the losses effectively reduce the S.I and the S.B of the spectra while the THG and the NFK increase them. However, the most deleterious factor for the Airy pulse is the LL, while that of the sech-type pulse is the TPA. The SCG spectra of the Airy pulse are broader than that of the sech-type in the studied waveguide; the intensity and area extent of the DWs are more important for the Airy pulse than the sech-type while the C.R is generated in the sech-type pulse because its spectrum is more affected by THG and NFK. Due to the presence of linear and nonlinear loss terms such as LL, FCA and TPA, the increase in signal energy is deleterious to the SCG in this silicon waveguide; this results in smaller spectra as peak power and pulse duration increase. The spectral coherence defined by the CD was found to be related to the previous result, i.e. when the pulse has more energy, the coherence decreases and therefore for the Airy pulse, the most consistent spectra are those under the LL effect alone and the most noisy spectra are those of NFK alone. It has also been shown that the Airy pulse has a spectral coherence above that of the sech-type pulse. Thus, for the realization of an optimal and more coherent SCG under the conditions described in this paper, the choice of an Airy pulse with short duration and low peak power is more suitable. Such features are expected to be useful in the SCG achievement through SOI-waveguides using Airy pulses for applications related to integrated chips and nanowires in all-optical systems.

Acknowledgments

S. K. Boukar is thankful to the scientific mobility scholarship offered by the French Embassy in Chad which allows him to complete his doctoral thesis in Cameroon and C. Heuteu thanks the C.E.T.I.C for the financial support during his thesis studies. All the the authors also acknowledge the support of the Optica Foundation for have waived the APC fees during the publication process in the Optics Express journal.

Disclosures

The authors declare that there are no conflicts of interest related to this paper.

See Supplement 1 for supporting content.

References

1. J. M. Dudley, G. Helsinki, and S. Coen, "Supercontinuum generation in photonic crystal fiber," Rev. Mod. Phys. **78**, 1135 (2006).
2. G. P. Agrawal, *Nonlinear Fiber Optics*, (Academic Press, California USA, 4th edn, 2007).
3. J. M. Dudley and J. R. Taylor, *Supercontinuum Generation in optical fibers* (Cambridge University Press, Cambridge, 1st ed., 2010).
4. G. P. Agrawal, *Applications of Nonlinear Fiber Optics*, (Academic Press, California USA, 2nd edn, 2008).

5. J. M. Dudley and S. Coen, "Coherence properties of supercontinuum spectra generated in photonic crystal and tapered optical fibers," Opt. Lett. **27**, 1180 (2002).
6. L. M. Mandeng, A. Mohamadou, C. Tchawoua, and H. Tagwo, "Spectral compression in supercontinuum generation through the higher-order nonlinear Schrödinger equation with non-Kerr terms using subnanojoule femtosecond pulses," J. Opt. Soc. Am. B **30**, 2555 (2013).
7. L. M. Mandeng, C. Tchawoua, H. Tagwo, M. Zghal, R. Cherif and A. Mohamadou, "Role of the Input Profile Asymmetry and the Chirp on the Propagation in Highly Dispersive and Nonlinear Fibers," Journal of Lightwave Technology **34**, 5635 (2016).
8. M. Diouf, L. M. Mandeng, C. Tchawoua, and M. Zghal, "Numerical Investigation of Supercontinuum Generation Through $AsSe_2/As_2S_5$ Chalcogenide Photonic Crystal Fibres and Rib Structures," J. Lightwave Technol. **37**, 5692-5698 (2019).
9. L. M. Mandeng, M. Diouf, C. Tchawa, and M. Zghal, "Mid-infrared broadband coherent supercontinuum spectrum in $AsSe_2/As_2S_5$ chalcogenide based waveguides," in Frontiers in Optics + Laser Science APS/DLS, The Optical Society (Optica Publishing Group, 2019), paper JW4A.60.
10. C. Heuteu, S. K. Boukar, L. M. Mandeng, and C. Tchawoua, "Supercontinuum generation of truncated Airy pulses in a cubic-quintic $AsSe_2/As_2S_5$ optical waveguide with rib-like structure," J. Opt. **23**, 095503 (2021).
11. L. M. Mandeng, C. Heuteu, S. K. Boukar, and C. Tchawoua, "Effects of nonlinear absorptions on Airy pulses supercontinuum in a cubic-quintic $AsSe_2/As_2S_5$ rib optical waveguide," in Frontiers in Optics + Laser Science 2021, C. Mazzali, T. (T.-C.) Poon, R. Averitt, and R. Kaindl, eds., Technical Digest Series (Optica Publishing Group, 2021), paper JTu1A.56.
12. L. M. Mandeng and C. Tchawoua, "Impact of input profile, absorption coefficients, and chirp on modulational instability of femtosecond pulses in silicon waveguides under fourth-order dispersion," J. Opt. Soc. Am. B **30**, 1382 (2013).
13. C. Ament, P. Polynkin, and J. V. Moloney, "Supercontinuum generation with femtosecond self-healing Airy pulses," Phys. Rev. Lett. **107**, 243901 (2011).
14. M. V. Berry and N. L. Balazs, "Nonspreading wave packets," Am. J. Phys. **47**, 264 (1979).
15. G. A. Siviloglou and D. N. Christodoulides, "Accelerating finite energy Airy beams," Opt. Lett. **32**, 979 (2007).
16. G. A. Siviloglou, J. Broky, A. Dogariu, and D. N. Christodoulides, "Observation of Accelerating Airy Beams," Phys. Rev. Lett. **99**, 213901 (2007).
17. J. Broky, G. A. Siviloglou, A. Dogariu, and D. N. Christodoulides, "Self-healing properties of optical Airy beams," Opt. Express **16**, 12880 (2008).
18. T. J. Eichelkraut, G. A. Siviloglou, I. M. Besieris, and D. N. Christodoulides, "Oblique Airy wave packets in bidispersive optical media," Opt. Lett. **35**, 3655 (2010).
19. P. Polynkin, M. Kolesik, J. Moloney, G. Siviloglou, and D. N. Christodoulides, "Curved Plasma Channel Generation Using Ultraintense Airy Beams," Opt. & Phot. News **21**, 38 (2010).
20. Y. Fattal, A. Rudnick, and D. M. Marom, "Soliton shedding from Airy pulses in Kerr media," Opt. Express **19**, 17298 (2011).
21. M. Asorey, P. Facchi, V. I. Man'ko, G. Marmo, S. Pascazio, and E. C. G. Sudarshan, "Generalized quantum tomographic maps," Phys. Rev. A **77**, 042115 (2008).
22. L. M. Mandeng and C. Tchawoua, in Frontiers in Optics Conference, "Nonlinear compression of self-healing Airy pulses in silicon-on-insulator waveguides," OSA Technical Digest (online) (Optical Society of America, 2012), paper FW3A.36.
23. L. M. Mandeng and C. Tchawoua, "Chirped self-healing Airy pulses compression in silicon waveguides under fourth-order dispersion," Journal of Modern Optics **60**, 359 (2013).
24. L. Mandeng Mandeng, S. Fewo Ibraid, C. Tchawoua, and T. C. Kofané, "A note on ultra-short pulses compression in silicon optical waveguides under fourth-order dispersion," Proc. SPIE 9286, Second International Conference on Applications of Optics and Photonics, 92863C (22 August 2014); https://doi.org/10.1117/12.2063573.
25. W. Liu, D. N. Neshev, I. V. Shadrivov, A. E Miroshnichenko, Y. S. Kivshar, "Plasmonic Airy beam manipulation in linear optical potentials," Opt. Lett. **36**, 1164 (2011).
26. P. Zhang, S. Wang, Y. Liu, X. Yin, C. Lu, Z. Chen, and X. Zhang, "Plasmonic Airy beams with dynamically controlled trajectories," Opt. Lett. **36**, 3191 (2011).
27. D. Abdollahpour, S. Suntsov, D. G. Papazoglou, and S. Tzortzakis, "Spatiotemporal airy light bullets in the linear and nonlinear regimes," Phys. Rev. Lett. **105**, 253901 (2010).
28. A. Chong, W. H. Renninger, D. N. Christodoulides, and F. W. Wise, "Airy?Bessel wave packets as versatile linear light bullets," Nat. Photonics **4**, 103 (2010).
29. W. Cai, M. S. Mills, D. N. Christodoulides, and S. Wen, "Soliton manipulation using Airy pulses," Optics Communications **316**, 127 (2014).
30. R. Driben, Y. Hu, Z. Chen, B. A. Malomed, and R. Morandotti, "Inversion and tight focusing of Airy pulses under the action of third-order dispersion," Opt. Lett. **38**, 2499 (2013).
31. W. Cai, L. Wang, and S. Wen, "Evolution of airy pulses in the present of third order dispersion," Optik **124**, 5833 (2013).
32. R. Driben and T. Meier, "Regeneration of Airy pulses in fiber-optic links with dispersion management of the two leading dispersion terms of opposite signs," Phys. Rev. A **89**, 043817 (2014).

33. L. M. Mandeng and C. Tchawoua, "Asymmetric inversion of Airy pulses induced by the interaction between the initial chirp and the group-velocity dispersion in a single mode fiber," in Frontiers in Optics Conference, OSA Technical Digest (online) (Optical Society of America, 2014), paper FTh4B.5.
34. L. Zhang, K. Liu, H. Zhong, J. Zhang, Y. Li, and D. Fan, "Effect of initial frequency chirp on Airy pulse propagation in an optical fiber," Opt. Express **23**, 2566 (2015).
35. C. Heuteu, L. M. Mandeng, and C. Tchawoua, "Chirp-dispersion management inducing regeneration of truncated Airy pulses in fiber optics links," J. Opt. Soc. Amer. B **37**, A121 (2020).
36. S. K. Boukar, C. Heuteu, L. M. Mandeng, and C. Tchawoua, "Modulational instability of truncated Airy pulses in cubic-quintic nonlinear optical waveguides with multiphoton absorptions," Optics Communications **521**, 128593 (2022).
37. S. K. Boukar, C. Heuteu, L. M. Mandeng, and C. Tchawoua, "Multiphoton absorptions effects on Airy pulses modulational instability in a cubic-quintic rib optical waveguide," in Frontiers in Optics + Laser Science 2022 (FIO, LS), Technical Digest Series (Optica Publishing Group, 2022), paper FTh3C.4.
38. A. Banerjee and S. Roy, "Collision-mediated radiation due to Airy-soliton interaction in a nonlinear Kerr medium," Phys. Rev. A **98**, 033806 (2018).
39. A. Banerjee and S. Roy, "Self-healing dynamics and absolute temporal focusing of a truncated Airy pulse under higher-order phase modulations," J. Opt. Soc. Amer. B **35**, 878 (2018).
40. Q. Lin, O. J. Painter, and G. P. Agrawal, "Nonlinear Optical Phenomena in Silicon Waveguides: Modeling and Applications," Opt. Express **15**, 16604 (2007).
41. L. Yin, Q. Lin, and G. P. Agrawal, "Soliton fission and supercontinuum generation in silicon waveguides," Opt. Lett. **32**, 391 (2007).
42. J. Wen, H. Liu, N. Huang, Q. Sun, and W. Zhao, "Influence of the initial chirp on the supercontinuum generation in silicon-on-insulator waveguide," Appl. Phys. B **104**, 867 (2011).
43. D. Castelló-Lurbe, E. Silvestre, P. Andrés, and V. Torres- Company, "Spectral broadening enhancement in silicon waveguides through pulse shaping," Opt. Lett. **37**, 2757 (2012).
44. N. Singh, D. D. Hudson, Y. Yu, C. Grillet, S. D. Jackson, A. Casas-Bedoya, A. Read, P. Atanackovic, S. G. Duvall, S. Palomba, B. Luther-Davies, S. Madden, D. J. Moss, and B. J. Eggleton, "Midinfrared supercontinuum generation from 2 to 6 μm in a silicon nanowire," Optica **2**, 797 (2015).
45. A. G. Griffith, R. K. W. Lau, J. Cardenas, Y. Okawachi, A. Mohanty, R. Fain, Y. H. D. Lee, M. Yu, C. T. Phare, C. B. Poitras, A. L. Gaeta, and M. Lipson, "Silicon-chip mid-infrared frequency comb generation," Nature Communications **6**, 6299 (2015).
46. B. Kuyken, T. Ideguchi, S. Holzner, M. Yan, T. W. Hänsch, J. V. Campenhout, P. Verheyen, S. Coen, F. Leo, R. Baets, G. Roelkens, and N. Picqué, "An octave-spanning mid-infrared frequency comb generation," Nature Communications **6**, 6310 (2015).
47. H. K. Tsang, C. S. Wong, and T. K. Liang, "Optical dispersion, two-photon absorption and self-phase modulation in silicon waveguides at 1.5 μ m wavelength," Appl. Phys. Lett. **80**, 416 (2002).
48. L. Yin and G. P. Agrawal, "Impact of two-photon absorption on self-phase modulation in silicon waveguides," Opt. Lett. **32**, 2031 (2007).
49. V. Nathan, A.H. Guenther, "Review of multiphoton absorption in crystalline solids," J. Opt. Soc. Amer. B **2**, 294 (1985).
50. F.E. Hernández, K.D. Belfield, I. Cohanoschi, M. Balu, K.J. Schafer, "Three- and four-photon absorption of a multiphoton absorbing fluorescent probe," Appl. Opt. **43**, 5394 (2004).
51. G.I. Stegeman, M. Liu, S. Polyakov, F. Yoshino, L. Friedrich, "Nonlinear optics of polydiacetylenes," Nonlinear Opt. **24**, 1 (2000).
52. W. Chen, S. Bhaumik, S. A. Veldhuis, G. Xing, Q. Xu, M. Grätzel, S. Mhaisalkar, N. Mathews, T.C. Sum, "Giant five-photon absorption from multidimensional core-shell halide perovskite colloidal nanocrystals," Nature Commun. **15198**, 1 (2017).
53. C. R. Loures, A. Armaroli, and F. Biancalana, "Contribution of third-harmonic and negative-frequency polarization fields to self-phase modulation in nonlinear media," Opt. Lett. **40**, 613 (2015).
54. M. Conforti, A. Marini, T. X. Tran, D. Faccio, and F. Biancalana, "Interaction between optical fields and their conjugates in nonlinear media," Opt. Express **21**, 31239 (2013).
55. E. Rubino, J. McLenaghan, S. C. Kehr, F. Belgiorno, D. Townsend, S. Rohr, C. E. Kuklewicz, U. Leonhardt, F. König, and D. Faccio, "Negative-Frequency Resonant Radiation," Phys. Rev. Lett. **108**, 253901 (2012).
56. E. Rubino, A. Lotti, F. Belgiorno, S. L. Cacciatori, A. Couairon, U. Leonhardt, and D. Faccio, "Soliton-induced relativistic-scattering and amplification," Sci. Rep. **2**, 932 (2012).
57. M. Conforti, N.Westerberg, F. Baronio, S. Trillo, and D. Faccio, "Negative-frequency dispersive wave generation in quadratic media," Phys. Rev. A **88**, 013829 (2013).
58. L. M. Mandeng, S. I. Fewo, and C. Tchawoua, "Four-wave mixing growth in wavelength-division multiplexing solitons systems near the zero-dispersion wavelength," Eur. Phys. J. D **67**, 30511 (2013).
59. L. Mandeng Mandeng, S. Fewo Ibraid, and C. Tchawoua, "Full model analysis of the four-wave mixing anti-STOKES component growth in the wavelength-division multiplexing solitons systems near the zero-dispersion wavelength", Proc. SPIE 8785, 8th Iberoamerican Optics Meeting and 11th Latin American Meeting on Optics, Lasers, and Applications, 8785AL (18 November 2013); https://doi.org/10.1117/12.2021714.

60. C. Run, J. Weiguo, W. Xuying, and L. Jiaqi, "Transmission characteristics of subpicosecond Airy pulses in silicon-on-insulator waveguides," J. Opt. Soc. Am. B **34**, 2295 (2017).
61. J. Lu, W. Jia, and M. Neimule, "Transmission characteristics of chirped Airy pulses in silicon-on-insulator waveguides," Optik **194**, 162845 (2019).
62. J. C. Travers, M. H. Frosz and J. M. Dudley, "Nonlinear fibre optics overview," (2009) in *Supercontinuum Generation in Optical Fibers*, 1st ed., Cambridge, U.K.: Cambridge Univ. Press, 2010.
63. Y. A. Vlasov and S. J. McNab, "Losses in single-mode silicon-on-insulator strip waveguides and bends," Optics Express **12**, 1622 (2004).
64. F. Leo, S.-P. Gorza, J. Safioui, P. Kockaert, S. Coen, U. Dave, B. Kuyken, and G. Roelkens, "Dispersive wave emission and supercontinuum generation in a silicon wire waveguide pumped around the 1550 nm telecommunication wavelength," Opt. Lett. **39**, 3623 (2014).
65. H. H. Li, "Refractive index of silicon and germanium and its wavelength and temperature derivatives," Journal of Physical and Chemical Reference Data **9**, 561 (1980).
66. K. L. Corwin, N. R. Newbury, J. M. Dudley, S. Coen, S. A. Diddams, K. Weber, and R. S. Windeler, "Fundamental noise limitations to supercontinuum generation in microstructure fiber," Phys. Rev. Lett. **90**, 113904 (2003).
67. G. Genty, S. Coen, and J. M. Dudley, "Fiber supercontinuum sources (Invited)," J. Opt. Soc. Am. B **24**, 1771 (2007).
68. S. Roy, S. K. Bhadra, and G. P. Agrawal, "Dispersive wave generation in supercontinuum process inside nonlinear microstructured fibre," Current Science **100**, 321 (2011).